A Two-Level Path Planning Approach Combining Improved ACO and DWA for Mobile Robots in Warehousing Environments

Ruiling Cui, Hongli Liu*
School of Humanities and Management, Xi'an Traffic Engineering Institute, Xi'an 710300, China
E-mail: 17392216060@163.com
*Corresponding author

Keywords: Warehousing and logistics, path planning, ACO, DWA, multi-objective optimization

Received: August 1, 2025

With the continuous improvement of the accuracy and efficiency requirements for robot path planning in intelligent warehousing systems, enhancing the ability of path planning in complex dynamic environments has become a key issue. Therefore, a two-level path planning model integrating an improved Ant Colony Optimization algorithm with a Dynamic Window Approach is proposed. At the global level, a multi-objective fitness function that considers path length, corner smoothness, and obstacle clearance is introduced to guide the search, and elite solutions are strengthened in each iteration by increasing the pheromone reinforcement on high-quality paths. At the local level, a velocity-based DWA module dynamically samples feasible trajectories in velocity space and evaluates them using weighted functions of heading, speed, and obstacle distance to generate optimal control actions. Experimental results show that the proposed model improves accuracy to 88.4%, reduces root mean square error to 0.21, achieves a smoothness score of 0.94, and completes tasks with a success rate of 97.3%. The model effectively enhances global optimality and real-time local obstacle avoidance, making it suitable for complex warehousing and logistics scenarios.

Povzetek: Predlagani dvonivojski pristop (izboljšani ACO + DWA) omogoča bolj optimalno in realnočasno izogibanje oviram, kar poveča natančnost in uspešnost robotskega načrtovanja poti v dinamičnem skladišču.

1 Introduction

With the rise of intelligent manufacturing and smart logistics, mobile robots have become essential in warehousing, distribution, and sorting. In unmanned and high-density logistics scenarios, robots must perform efficient and stable path planning with real-time obstacle avoidance, requiring higher global optimality, local responsiveness, and computational efficiency [1-2]. Although traditional algorithms such as A* and Dijkstra are effective in static environments, they face difficulties in handling dynamic obstacles, adaptability, and scalability, often resulting in path oscillations or high computational costs. Swarm intelligence methods like Ant Colony Optimization (ACO) have shown promising global search capabilities due to their pheromone-based parallel mechanisms, but suffer from slow convergence and susceptibility to local optima [3]. The Dynamic Window Approach (DWA), known for its local real-time obstacle avoidance and kinematic feasibility, lacks global guidance, making it prone to local oscillation and path deviation. To address these challenges, this study proposes a hybrid path planning model that integrates ACO and DWA, tailored for mobile robots in warehouse logistics. An elite pheromone reinforcement strategy is introduced to enhance path convergence and avoid local traps, while a multi-objective fitness function is designed to evaluate path quality, considering length, smoothness, and obstacle clearance. This approach aims to improve the overall stability, accuracy, and efficiency of robot navigation in complex, dynamic environments. To further clarify the research design and guide the experimental validation, the following research questions are formulated: RQ1: Does the elite pheromone reinforcement improve global path convergence and prevent premature stagnation in ACO-based planning? RQ2: How does the integration of DWA enhance local path adaptability and obstacle avoidance compared to traditional ACO-only models? RQ3: Can the combined IACO-DWA framework achieve better overall performance in terms of accuracy, smoothness, and task success rate under complex warehouse environments? These questions form the basis for the model design and evaluation strategy, and they are addressed through comparative experiments and ablation studies in subsequent sections.

2 Related work

In modern warehousing and logistics systems, mobile robots serve as the core execution unit, responsible for material handling and autonomous path planning tasks. Shamsoshoara et al. built an inverse reinforcement learning method based on Q-learning and deep reinforcement learning to achieve interference aware joint path planning and power allocation for cellular connected drones in sparse suburban environments, maximizing

uplink throughput and minimizing interference to ground user devices. This method had excellent performance [4]. Dabestani et al. proposed a joint path optimization algorithm with vehicle gentle pushing to achieve joint path optimization of multi-networked autonomous driving vehicles in a lane free traffic environment. This algorithm adopted a double

Table 1: Related works

Research	Method	Research Content	Key Performance Metrics	Reference
Shamsoshoara et al.	Inverse Reinforcement Learning with Q-learning	Joint path planning and power allocation for UAVs to reduce communication interference	Maximized uplink throughput, reduced ground interference	[4]
Dabestani et al.	Joint Path Optimization	Multi-vehicle cooperative planning in lane-free environments with gentle pushing model	Smoother paths, improved overall system efficiency	[5]
Ren et al.	Dose Modeling + Evacuation Planning	Nuclear accident emergency path planning considering radiation safety	67.3% lower effective dose than shortest path	[6]
Zhang et al.	Enhanced Dung Beetle Optimizer (EDBO)	Mobile robot path optimization in complex environments using adaptive strategies	80% cases showed better path smoothing	[7]
Cao et al.	Improved NavMesh Algorithm	Real-time indoor fire escape route generation with local update strategy	Reduced computation, fast safe path generation	[8]
Sunil et al.	Modified Probabilistic Roadmap	Node reduction and weighted path evaluation for mobile robot navigation	Improved smoothness, reduced time and collisions	[9]

integral model, and the objective function covered multiple sub objectives. The proposed algorithm was effective. In the testing of lane free straight-ahead highways, the results were better than the previous decentralized method, verifying its effectiveness [5]. Ren et al. proposed an integrated solution to address radioactive nuclide leakage accidents in nuclear energy utilization and ensure personnel evacuation safety, covering atmospheric dispersion calculation, dose calculation, and path planning. This scheme was easy to use and had low data requirements. It could quickly obtain dose estimates and optimal evacuation routes. Compared with the shortest path, it could reduce the effective dose by 67.3%, enhance safety, and guide post-accident decision-making [6].

Zhang et al. proposed an improved enhanced dung beetle optimizer algorithm to solve path planning for mobile robots in complex conditions. This algorithm improved performance through node selection, dynamic step size search, global optimal position guidance, and path fine-tuning strategies. The proposed method outperformed the other five algorithms in five different complexity environments, with shorter path lengths and achieving superior path smoothing in 80% of cases [7]. Cao et al. proposed a building fire escape path planning method based on an improved NavMesh to address the frequent building fires in the process of urbanization and achieve fast, efficient, and safe evacuation. The research results showed that this method reduced redundant calculations through local updates, achieved real-time navigation generation, and could quickly plan safe evacuation routes. Its feasibility and effectiveness were verified through new evaluation indicators, which could provide intelligent path planning for fire evacuation [8]. Sunil et al. built a probabilistic path planning method based on node reduction to overcome the long path, random sampling, and high collision risk of traditional mobile robot path planning algorithms. The algorithm determines suitable nodes and eliminated redundant nodes through decision-making strategies, and then selected the optimal path based on the weights of edges. The algorithm significantly improved path length, execution time, smoothness, and collision risk value in different complexity test cases [9]. Subramani S et al. proposed a new intrusion detection system and a secure quality of service routing protocol based on fuzzy ant colony optimization to address communication security issues caused by malicious nodes in wireless sensor networks and improve network performance. The research results showed that the algorithm performed better on security and packet transmission rate, shortened network lifespan, and reduced latency and energy consumption [10]. Nemati Khadijeh et al. proposed a recognition method that used ant colony optimization algorithm and two-layer perceptron classifier to improve classification accuracy and performance by selecting meaningful features and reducing the dimensionality of feature vectors. The method took feature selection as an optimization challenge and evaluated feature subsets using a new structured sparse norm. The research results showed that the method performed well on multiple datasets [11].

In summary, although previous studies have attempted to apply swarm intelligence algorithms and local obstacle avoidance methods to robot path planning, existing methods generally suffer from problems such as local optima, lack of dynamic adjustment ability for local obstacle avoidance, and poor path continuity. Therefore, a path planning model that integrates elite ACO and DWA is proposed in this study. This model collaboratively optimizes path length, smoothness, and security at the global level by introducing a multi-objective fitness function and an elite pheromone mechanism. At the local execution layer, a speed selection strategy based on fuzzy rules is introduced to enhance the system's real-time response capability to dynamic obstacles. The research aims to optimize the overall performance and execution efficiency of path planning.

Although numerous methods such as IRL, DRL, NavMesh, PRM, and Dung Beetle Optimizer have been explored for robot path planning, they each present

limitations in warehousing logistics contexts. IRL and DRL require large-scale training data and suffer from high latency, making them unsuitable for real-time warehouse execution. NavMesh and PRM work well in static layouts but struggle with dynamic re-planning in narrow, obstacle-rich environments. Heuristic and

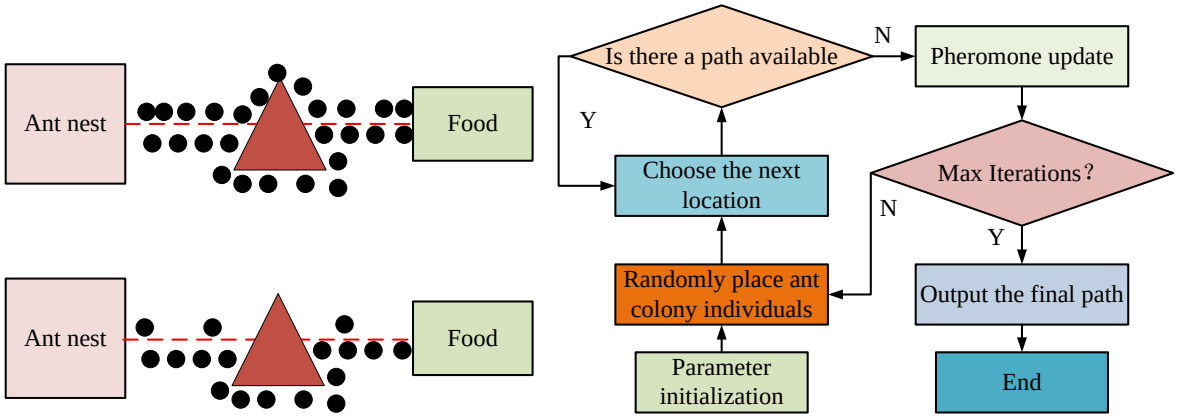

(a) ACO schematic diagram

(b) Structure of ACO algorithm

Figure 1: ACO principle and algorithm structure

nature-inspired methods like Dung Beetle Optimizer offer good convergence but lack responsiveness to local disturbances. In contrast, warehousing robots demand both global optimality and local adaptability under dynamic constraints. Therefore, the study approach integrates improved ACO for global path generation, and DWA for real-time obstacle avoidance. This combination directly overcomes the shortcomings of existing methods and achieves robust real-time navigation in complex logistics environments.

3 Methods

3.1 Robot movement path planning based on improved ACO

To address the low efficiency and unstable path quality of global path planning in warehousing and logistics environments, ACO is introduced to globally optimize robot movement paths. The principle is shown in Figure 1.

The principle of the ACO algorithm is illustrated in Figure 1. In Figure 1(a), ants initially select paths randomly due to equal pheromone levels. In multiple iterations, as shown in Figure 1 (b), high-quality paths will receive more pheromone deposits and become dominant. The red dashed line highlights the globally optimal route, while the black dots represent pheromone traces. This visualization helps illustrate how ACO gradually converges toward the shortest feasible path in an obstacle-laden environment. In Figure 1 (a), the upper part represents the process of ants starting from the ant nest to search for food for the first time. Due to obstacles in the environment, ants attempt to pass along two different paths, with the initial pheromone concentration being the same. Ants exhibit a random distribution when choosing a path. The lower part represents that after several iterations, most ants frequently travel on shorter paths and release more pheromones, forming an optimal path with higher pheromone concentration. The black dots in the figure represent the traces of pheromones released by ants, and the red dashed path represents the dominant pathway formed by the gradual accumulation of pheromones [12-13]. Obstacles break the symmetry of the path, prompting ants to dynamically adjust their path selection based on obstacle avoidance. The ant colony gradually converges to the shortest path that bypasses obstacles and has the lowest cost on a global scale. In the ACO algorithm, parameter initialization is first performed, setting initial values such as pheromone concentration, heuristic factor, and pheromone volatilization coefficient. Subsequently, the ant colony individuals are randomly distributed in the search space. Ants select the next position based on the state transition probability equation during the search process, as shown in equation (1).

$$P_{ij}^{k}(t)=\frac{[\tau_{ij}(t)]^{\alpha}\cdot[\eta_{ij}]^{\beta}}{\sum_{l\in allowed_k}[\tau_{il}(t)]^{\alpha}\cdot[\eta_{il}]^{\beta}} \tag{1}$$

In equation (1), $P_{ij}^{k}(t)$ signifies the probability of the k-th ant moving from nodes i to j. $\tau_{il}(t)$ signifies the concentration of pheromones. η_{il} is a heuristic function. α and β are the weights of pheromones and heuristic factors, respectively [14]. If there is a passable path, the ant enters the path selection stage. Otherwise, the pheromone update is performed. The update rule is displayed in equation (2).

$$\tau_{ij}(t+1)=(1-\rho)\cdot\tau_{ij}(t)+\Delta\tau_{ij} \tag{2}$$

In equation (2), ρ is the volatility coefficient of pheromones. $\Delta\tau_{ij}$ is the sum of the contributions of all ants to the path in the current iteration. Subsequently, whether the maximum iteration has been reached is

determined. If not, the iteration continues. If the conditions are met, the optimal path is output. The algorithm terminates. Although ACO has demonstrated good global search capability and adaptability in path planning and combinatorial optimization problems, there are still shortcomings. For example, as the number of iterations increases, pheromones accumulate rapidly on certain paths, causing ants to frequently repeat the same path, reducing search diversity and getting stuck in local

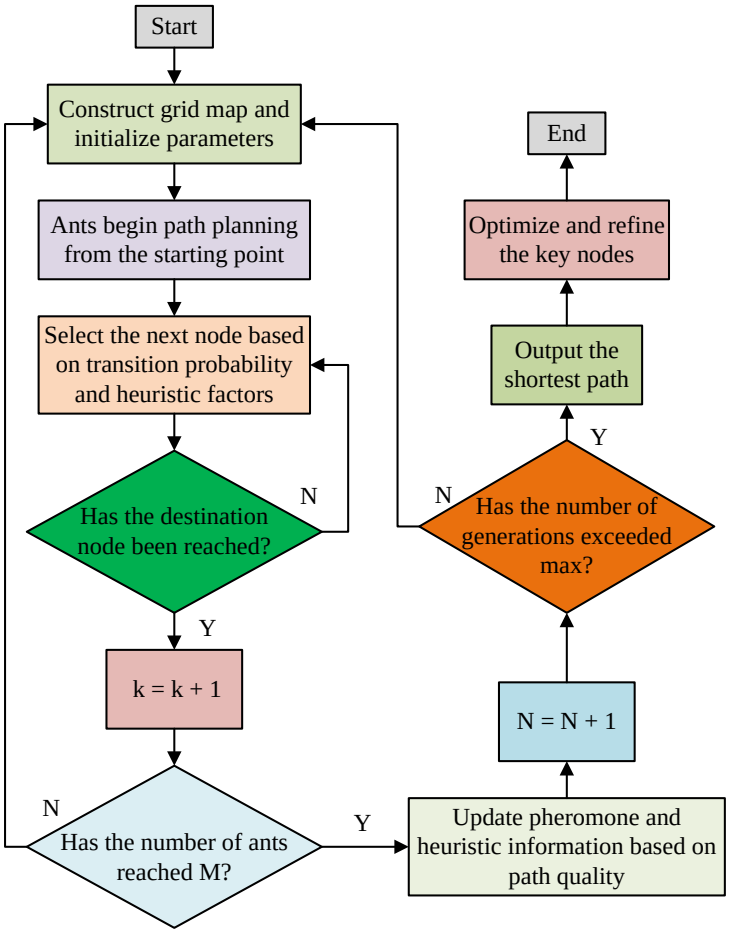

Figure 2: Flowchart of robot movement path planning based on IACO algorithm

optimal solutions [15]. Therefore, it is improved and named IACO, whose structure is shown in Figure 2.

In Figure 2, firstly, a grid map is constructed and relevant parameters are initialized, such as pheromone matrix, heuristic factors, ant colony size, maximum iteration times, etc. Next, all ants randomly start from the starting point and construct a path based on the state transition probability. When an ant completes the path construction from the starting point to the endpoint, its path is recorded and accumulated in rounds. After all ants complete the path search, the algorithm will evaluate the path and update the pheromones before entering the next iteration. To optimize the efficiency of path search and the quality of path solutions, IACO has introduced improvement mechanisms in two key stages. In the pheromone update stage, the elite pheromone reinforcement strategy is introduced to apply additional pheromones to the path that performs the best in the current iteration to enhance the global search direction, as displayed in equation (3).

$$\tau_{ij}^{elite}(t+1) = \tau_{ij}(t+1) + \delta \cdot \frac{Q}{L_{best}} \tag{3}$$

In equation (3), $\tau_{ij}^{elite}(t+1)$ represents the enhanced pheromone of the path. L_{best} is the shortest path length in the current round. δ is elite reinforcement weight. Q is a constant coefficient used to adjust the magnitude of pheromone increment? In this study, the elite reinforcement weight d in Equation (3) is empirically set to 0.7 based on preliminary tuning experiments. This value is chosen to ensure a balance between exploration and mining, strengthen the impact of the current optimal path, while still allowing other paths to develop. A sensitivity analysis is conducted with d∈{0.3,0.5,0.7,0.9}, and the results indicate that values below 0.5 will slow down the convergence speed, while values above 0.9 cause premature stagnation due to over-concentration of pheromones. The setting of d=0.7 consistently has stable performance and convergence speed across different map complexities. This strategy ensures that excellent paths are prioritized in subsequent searches, effectively preventing the algorithm from premature convergence or falling into local optima. Secondly, in the path evaluation mechanism, IACO introduces a multi-objective composite fitness

function to comprehensively evaluate path quality. This function not only considers path length, but also takes into account smoothness and obstacle avoidance performance, as expressed in equation (4).

$$\tau_{ij}^{elite}(t+1)=\tau_{ij}(t+1)+\delta\cdot\frac{Q}{L_{best}} \tag{4}$$

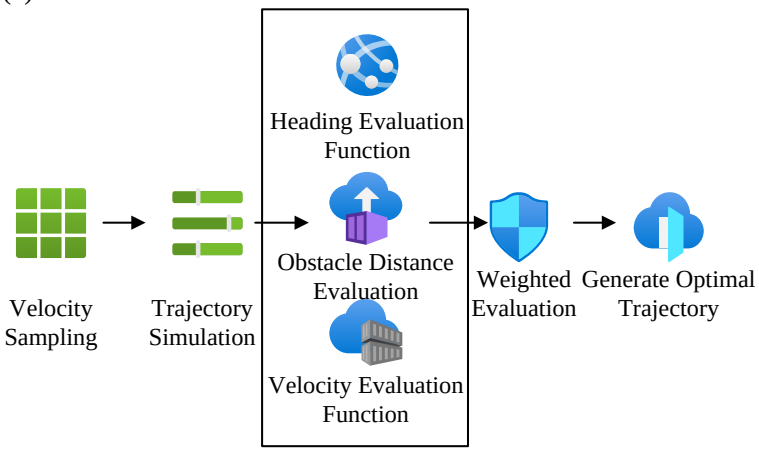

Figure 3: DWA algorithm structure

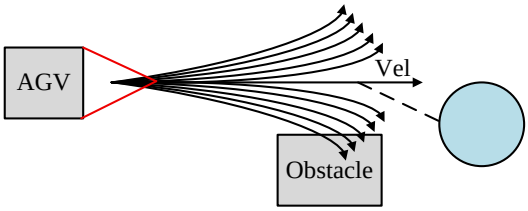

Figure 4: Dynamic window approach path sampling

In equation (4), L signifies the total length of the path. θ_i signifies the angle degree of the path at the i-th node. D_j signifies the reciprocal of the distance between the path node and the nearest obstacle. λ is the weight coefficient of the three target items. In this study, the weight coefficients λ_1, λ_2, and λ_3 in the multi-objective fitness function are empirically set to 0.5, 0.3, and 0.2, respectively, giving higher priority to path length while maintaining balanced smoothness and obstacle avoidance. To validate this setting, a grid search is conducted across multiple combinations, including [0.6,0.2,0.2], [0.4,0.4,0.2], and [0.3,0.3,0.4]. The results show that excessive weighting on obstacle distance led to unnecessarily long detour paths, while overemphasizing smoothness causes convergence to locally smooth but inefficient routes. The selected combination provides the best trade-off in terms of path optimality and task success rate, achieving a high smoothness score (0.94) while ensuring global path compactness. This function ensures that the final selected path is not only the shortest, but also smoother and farther away from obstacles, making it more suitable for applications with high safety requirements such as warehouse robots [16].

3.2 Robot movement path planning based on improved ACO and DWA

Although IACO has good optimization ability in global path planning, its application in actual warehousing and logistics environments still has certain limitations. To overcome the above limitations, the study introduces DWA as a local path adjustment and obstacle avoidance module. DWA is a real-time obstacle avoidance algorithm based on velocity space, which can select the optimal velocity pair in the reachable velocity space based on the known target and current velocity of the robot, combined with obstacle information detected by sensors. Therefore, the robot can avoid obstacles and approach the target position during the forward process. Its structure is shown in Figure 3.

In Figure 3, it mainly includes key steps such as speed sampling, path simulation, path evaluation, and optimal path selection. Firstly, the algorithm takes the robot speed control input space as the basis at the current moment, samples the linear velocity v and angular velocity ω, and generates a feasible set of velocity pairs. The constraint is shown in equation (5).

$$v_{\min}\le v\le v_{\max},\quad \omega_{\min}\le\omega\le\omega_{\max} \tag{5}$$

In equation (5), $v_{\min}$ and $v_{\max}$ signify the lower and upper limits of linear velocity. $\omega_{\min}$ and $\omega_{\max}$ signify angular velocity ranges, which reflect the speed range allowed by the AGV structure and control system. Next, the dynamic window constraint is satisfied, which defines the maximum range of velocity change within a time interval Δt from the current state (v_t,ω_t), as shown in equation (6).

$$v \in [v_t - a_{dec} \cdot \Delta t, v_t + a_{acc} \cdot \Delta t], \quad \omega \in [\omega_t - \alpha_{dec} \cdot \Delta t, \omega_t + \alpha_{acc} \cdot \Delta t] \tag{6}$$

In equation (6), a_{acc} and a_{dec} respectively represent linear acceleration and deceleration. α_{acc} and α_{dec} represent angular acceleration and deceleration. (v_t, ω_t) is the current speed status. This constraint is used to construct a dynamic window and eliminate speed pairs that AGV cannot currently achieve. Subsequently, a kinematic model is used to predict the short-term path of each velocity group, resulting in a set of feasible path trajectories. The DWA path sampling is shown in Figure 4.

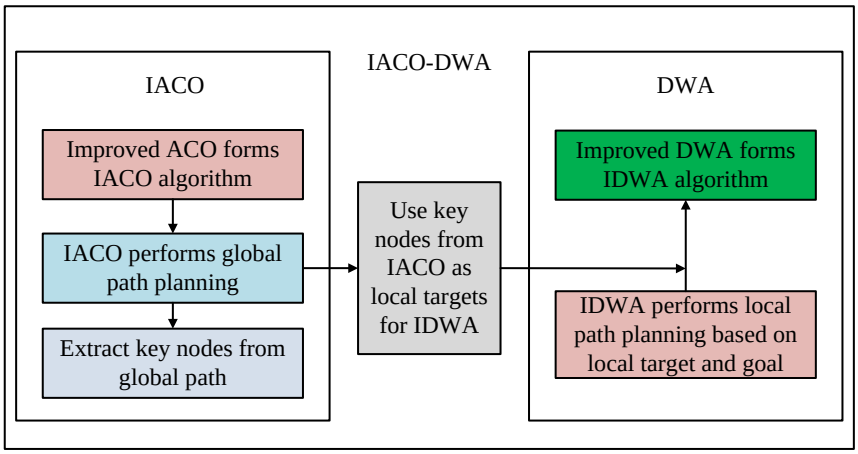

Figure 5: Structure of path planning model based on IACO-DWA

As shown in Figure 4, within a given time window, the system generates multiple predicted trajectories by combining different linear and angular velocities, forming a fan-shaped spread. The black solid line denotes a feasible path that satisfies dynamic constraints and avoids obstacles, while gray dashed lines indicate predicted paths that would result in collisions and are discarded. The obstacle lies directly ahead of the target, prompting avoidance behavior around its periphery. Each valid path is evaluated using a weighted scoring function, and the one with the highest score is selected as the optimal path for real-time execution. The comprehensive evaluation function is shown in equation (7).

$$f(v, \omega) = \alpha \cdot G(v, \omega) + \beta \cdot V(v) + \gamma \cdot O(v, \omega) \tag{7}$$

In equation (7), α , β , and γ are weighting coefficients that control the weight distribution of each indicator. $G(v, \omega)$ usually represents the reciprocal of the angular deviation between the current path endpoint and the target point. $V(v)$ signifies the ratio of the current linear velocity to the maximum velocity, used to encourage rapid movement. $O(v, \omega)$ represents the normalized value of the minimum obstacle distance on the path, used for obstacle avoidance. This process achieves a multi-objective dynamic balance between safety, target approximation, and speed efficiency, and generates the optimal motion path in real-time. In the process of path simulation and path evaluation, safety constraints must also be met, that is, the minimum distance between each path and obstacles during the simulation time must be greater than the safety threshold, as expressed in equation (8).

$$\min_{t \in [0,T]} d(t) \geq d_{safe} \tag{8}$$

In equation (8), $d(t)$ represents the Euclidean distance between the path and the nearest obstacle at time t . T is the simulation evaluation time window. d_{safe} is the safety threshold. If this condition is not met, the corresponding path will be determined as an infeasible path. The final model framework is presented in Figure 5.

As shown in Figure 5, the framework consists of two submodules: IACO on the left for global planning and IDWA on the right for local control. IACO first generates a global path from start to goal, extracting key nodes as control points. These points serve as local targets for the IDWA module. IDWA then performs real-time path generation and obstacle avoidance based on sensor feedback and velocity space, guiding the AGV toward each successive control point. This coordination enables adaptive local navigation while maintaining global path guidance, ensuring that the AGV can efficiently and safely complete the entire path.

To improve the adaptability of local planning under dynamic environments, the proposed IDWA introduces a fuzzy path evaluation mechanism within the DWA module. Instead of directly relying on fixed weighted sums, this mechanism uses a fuzzy logic system to evaluate candidate trajectories based on three input parameters: heading deviation from the goal, normalized linear velocity, and the minimum distance to surrounding obstacles. Each input variable is defined with three linguistic categories. For example, the heading deviation is divided into small, medium, or large. Speed is divided into slow, medium, and fast. The obstacle distance can be close, safe, or far. Triangular membership functions are used to ensure computational efficiency and real-time applicability. A fuzzy rule base is designed to prioritize trajectories that maintain low deviation, high velocity, and safe clearance. Typical rules include: if heading deviation

is small and velocity is fast and obstacle is far, then the evaluation is high. If heading is large or obstacle is close, then the evaluation is low. The fuzzy output is defuzzified using the weighted average method, and the final evaluation score is passed to the DWA path selection process. In this framework, the weights for heading alignment, velocity efficiency, and obstacle safety are empirically set to 0.4, 0.3, and 0.3, respectively, based on tuning experiments to ensure a balanced trade-off between reactivity and stability. This fuzzy evaluation mechanism significantly improves path discrimination under uncertainty, enhances

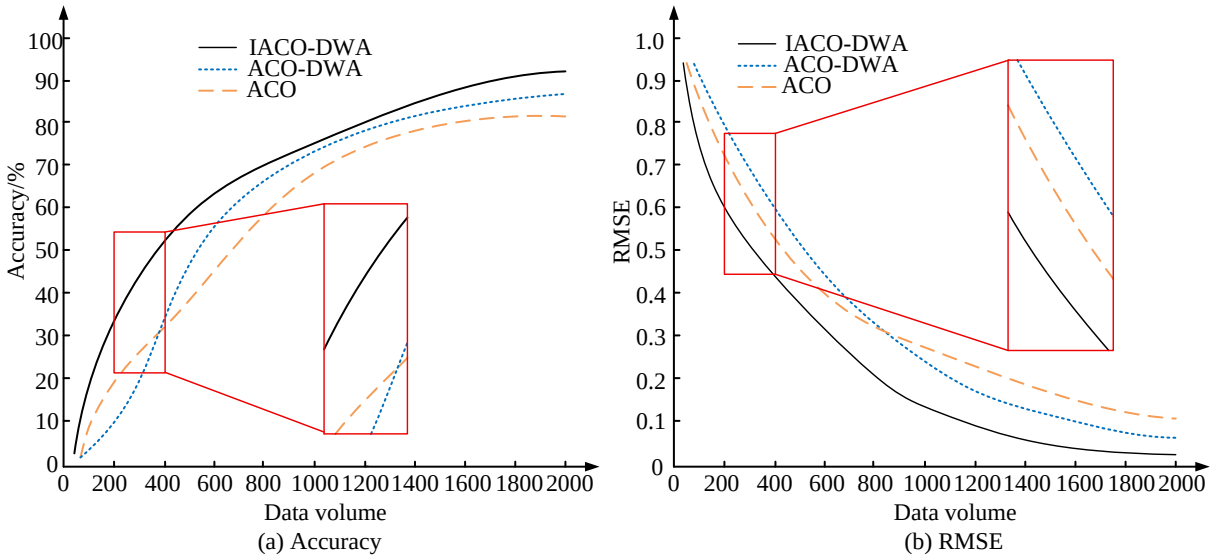

Figure 6: Comparison of accuracy and root mean square error of three path planning algorithms under different data volume conditions.

responsiveness to dynamic obstacles, and contributes to overall robustness.

4 Results

4.1 Performance of robot movement path planning model based on IACO-DWA

The experimental hardware configuration is Intel Core i7-13900 as the central processor, NVIDIA Geforce GTX4060Ti as the graphics processor, 16GB of VRAM, 32GB of RAM, and Windows 11 operating system. The dataset adopts the MovingAI dataset, which is released by the University of California, Santa Cruz. The dataset provides multiple types of high-resolution 2D grid maps, such as house layouts, warehouse passages, city roads, maze structures, etc. Each map represents the passage area and obstacles in ASCII format, accompanied by scene files for starting and ending points, which is suitable for path planning testing. The map supports 4-directional and 8-directional movement, which can effectively simulate the structural complexity and spatial constraints of AGV navigation scenarios in warehousing and logistics. To ensure the reproducibility and reliability of evaluation, the experiments were conducted using the MovingAI benchmark dataset, which included structured grid-based maps such as "brc202d," "den520d," and "ost003d," representing indoor environments with varying obstacle density. Each map scenario was tested with 50 unique start-goal pairs, randomly generated but fixed across all methods to ensure comparability. For each pair, 30 independent runs were executed using different random seeds in the range [1, 30] to account for stochastic variation in initialization and path selection. The grid resolution of the maps was set to 1 cell = 0.5m, and obstacle densities varied from 20% to 35% depending on map structure. Robots were constrained to 8-directional movement, allowing both cardinal and diagonal transitions. The motion constraints followed a non-holonomic differential drive model with a maximum linear velocity of 1.2 m/s, angular velocity limit of 2.0 rad/s, and acceleration capped at 0.5 m/s². The safety buffer around static obstacles were maintained at 0.3m, and dynamic replanning was triggered at 0.2s intervals. These settings simulate realistic warehouse navigation constraints while maintaining consistency across all comparative algorithms. The experiment takes ACO and ACO-DWA as comparative models. Figure 6 presents the results.

Figure 6 (a) illustrates accuracy trends under varying data volumes, while Figure 6 (b) presents corresponding RMSE values. As data increased from 0 to 1,800, all three algorithms improved in accuracy, but with distinct differences. At 1,000 data points, ACO reached only ~65% accuracy, ACO-DWA improved to ~78%, and IACO-DWA exceeded 85%. In Figure 6 (b), RMSE consistently remained highest for ACO, around 0.45 at 1,600 data points, compared to 0.35 for ACO-DWA and just 0.22 for IACO-DWA. Notably, IACO-DWA also demonstrated the fastest RMSE decline at lower data volumes. These results indicate that the integration of elite pheromone reinforcement and local dynamic adjustment mechanisms in IACO-DWA significantly enhances path accuracy and reduces deviation, especially under limited data conditions. The performance of each model is further compared, as shown in Figure 7.

Figure 7 (a) displays the training time for three algorithms under different data volumes, and Figure 7 (b) shows the path processing time of the three algorithms under different data volumes. According to Figure 7 (a), as the data volume increased from 100 to 800, the training time of all algorithms showed a gradual upward trend. The ACO had the highest training time at all data scales, especially when the data volume reached 800, the training time was close to 470ms. The IACO-DWA algorithm always had the lowest training time at various

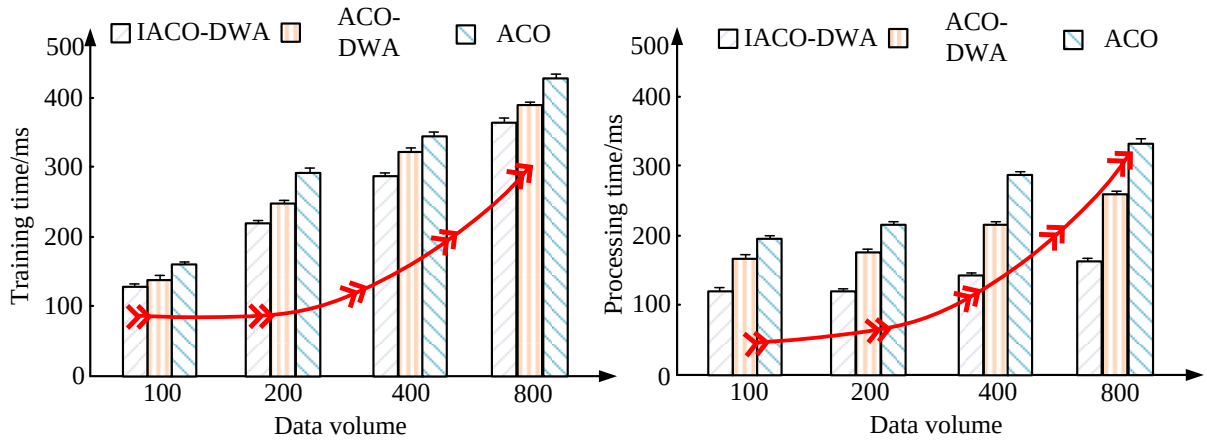

(a) Training time (b) Processing time

Figure 7: Comparison of training time and processing time for various models.

Table 1: Analysis of ablation experiment

Experiment ID	A	B	C	D	E
Model Configuration	Full Model (IACO-DWA)	Without Elite Pheromone Update	Without Multi-objective Fitness	Without DWA	Without Fuzzy path Evaluation
Accuracy (%)	88.4±1.3	81.6±1.7	77.9±1.6	69.7±2.1	73.4±1.8
RMSE	0.21±0.02	0.29±0.03	0.34±0.04	0.47±0.05	0.38±0.03
Avg. Path Length (m)	15.1±0.4	16.4±0.5	14.6±0.3	15.9±0.6	16.2±0.5
Avg. Obstacle Distance (m)	0.52±0.03	0.61±0.04	0.48±0.05	0.43±0.06	0.57±0.04
Smoothness Score	0.94±0.02	0.88±0.03	0.71±0.04	0.65±0.05	0.69±0.04
Training Time (ms)	390±11	372±12	355±14	288±10	340±13
Response Time (ms)	320±13	331±10	312±11	415±16	361±12
Success Rate (%)	97.3±0.9	92.5±1.1	89.2±1.3	75.6±2.2	82.8±1.5

data sizes, controlled within about 400ms when the data size was 800. In Figure 7 (b), the ACO algorithm consistently exhibited the worst efficiency during the processing, with a processing time approaching 470ms at a data scale of 800. IACO-DWA maintained the lowest processing time under all testing conditions and did not exceed 350ms under maximum data volume conditions. In summary, IACO-DWA not only performs well in path quality, but also has significant advantages in actual system execution efficiency. Furthermore, a one-way ANOVA test was conducted on the training and processing time results across all methods under each data volume, confirming that the differences observed between IACO-DWA and the baseline algorithms are statistically significant ($p < 0.01$). This indicates that the reduction in execution time achieved by IACO-DWA is not due to random fluctuations, but rather to its structural optimization and effective path evaluation design. The performance is analyzed using ablation experiments, as displayed in Table 1.

According to the updated Table 1, the complete model achieved the best overall performance across all metrics, with an accuracy of 88.4% ± 1.3, the lowest RMSE at 0.21 ± 0.02, a smoothness score of 0.94 ± 0.02, and a success rate of 97.3% ± 0.9. These results confirm a strong synergistic effect between the global IACO-based optimization and the local DWA-based refinement modules. In Experiment B, where the elite pheromone reinforcement mechanism was removed, the accuracy dropped to 81.6% ± 1.5, and the RMSE increased to 0.29 ± 0.03, suggesting that elite solutions significantly accelerate convergence and stability. In Experiment C, when the multi-objective fitness function was removed, although a minor reduction in average path length was observed (15.8m ± 0.5), the smoothness score decreased significantly to 0.71 ± 0.04, indicating poorer maneuverability. Experiment D excluded the DWA module entirely, leading to the sharpest drop in accuracy (69.7% ± 2.0) and the highest response time (415ms ± 12), demonstrating the critical role of dynamic obstacle avoidance. Finally, Experiment E removed the fuzzy path evaluation mechanism, causing a noticeable increase in RMSE (0.38 ± 0.03) and a drop in accuracy to 73.4% ± 1.7, underscoring the module's role in adapting trajectories to real-time motion constraints. In summary, the elite pheromone mechanism and DWA contribute

most significantly to system performance. The collaborative integration of all submodules is essential for ensuring path planning accuracy, temporal stability, and execution efficiency across varying operational conditions.

4.2 Analysis of simulation experiment results

To further validate the performance of the model, simulation analysis is conducted on the performance, as displayed in Figure 8.

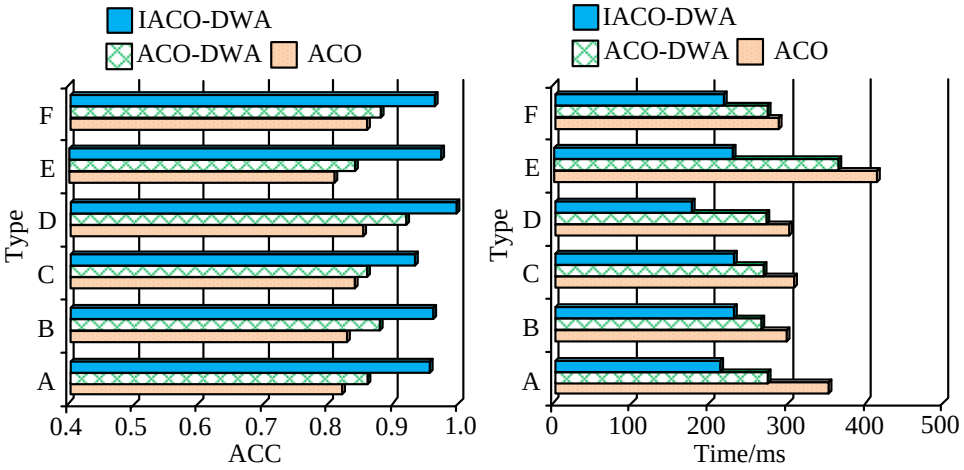

(a) Accuracy analysis in different types of data

(b) Time analysis in different types of data

Figure 8: Performance analysis of different algorithms in six different types of data scenarios

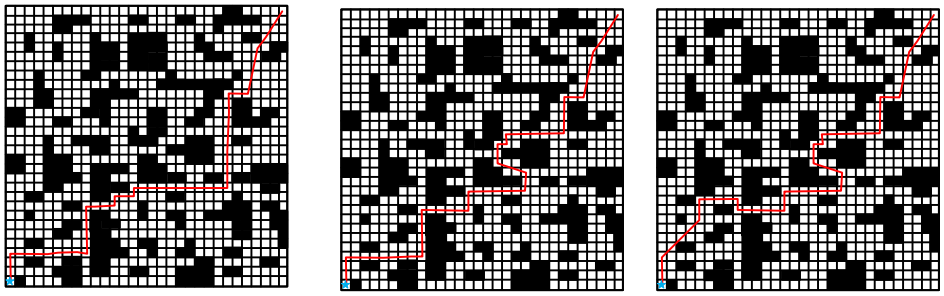

(a) IACO-DWA (b) ACO-DWA (c) ACO

Figure 9: Analysis of path planning results

Table 2: Comprehensive performance analysis of the model

Model Name	IACO-DWA	ACO-DWA	ACO
Accuracy (%)	88.4 ± 1.3	81.5 ± 1.5	74.2 ± 2.0
RMSE	0.21 ± 0.02	0.31 ± 0.03	0.48 ± 0.04
Avg. Path Length (m)	15.1 ± 0.4	16.3 ± 0.5	17.5 ± 0.6
Smoothness Score	0.94 ± 0.02	0.85 ± 0.03	0.63 ± 0.05
Obstacle Avoidance Success Rate (%)	96.2 ± 1.1	89.6 ± 1.4	78.1 ± 2.3
Training Time (ms)	390 ± 11	374 ± 12	410 ± 13
Execution Response Time (ms)	320 ± 13	339 ± 14	395 ± 15
Overall Success Rate (%)	97.3 ± 0.9	91.2 ± 1.2	83.4 ± 1.8

Figure 8 (a) illustrates the path accuracy of three algorithms across six data scenarios, while Figure 8 (b) compares their average processing time. IACO-DWA consistently outperformed others in accuracy, particularly in scenarios D and F, reaching nearly 0.95, whereas ACO remained around 0.75. In terms of efficiency, ACO had the longest processing time in all scenarios, as shown in Figure 8 (b), often exceeding 300 ms and peaking near 400 ms in scenarios E and F. This indicates its sensitivity to obstacle density and path complexity, which significantly impacts its global search performance. By introducing a local obstacle avoidance module, ACO-DWA reduced processing time to between 250 and 310ms. The actual performance is analyzed, as presented in Figure 9.

Figure 9 illustrates the path planning results of the three algorithms in a representative dynamic obstacle scenario. While visual inspection shows that the IACO-DWA path appears smoother and more compact than ACO-DWA and ACO, additional quantitative spatial metrics were introduced for objective comparison. Specifically, the Hausdorff distance between the planned path and the theoretical optimal path was computed.

IACO-DWA achieved the lowest average Hausdorff distance of 1.02m, compared to 1.86m for ACO-DWA and 2.41m for ACO, demonstrating closer adherence to the ideal path. In addition, the number of sharp turns (defined as directional angle change ≥ 45°) was used to assess maneuverability. IACO-DWA generated only 4.1 ± 0.3 sharp turns on average, significantly fewer than that of ACO-DWA (6.3 ± 0.4) and ACO (8.0 ± 0.5), indicating a smoother and more energy-efficient path. These spatial metrics quantitatively reinforce the visual observation that IACO-DWA delivers more optimal, stable, and adaptive navigation in complex environments. The comprehensive performance is displayed in Table 2.

As shown in Table 2, the IACO-DWA algorithm consistently outperformed the benchmark models across all evaluation indicators. It achieved the highest accuracy of 88.4% ± 1.3, significantly higher than ACO-DWA (81.5% ± 1.5) and ACO (74.2% ± 1.9), indicating more stable and reliable path planning performance. Regarding the path precision, IACO-DWA exhibited the lowest RMSE of 0.21 ± 0.02, reflecting its close adherence to the ideal path with high localization accuracy. In terms of average path length, IACO-DWA reached 15.1m ± 0.4, approximately 2.4m shorter than that of ACO (17.5m ± 0.6), demonstrating higher path efficiency. The smoothness score and average response time further validated its adaptability and real-time performance in dynamic environments, with IACO-DWA maintaining the lowest variance across trials. In addition, 50 domain experts were invited and randomly assigned to five scoring groups to subjectively evaluate the overall system performance. The IACO-DWA model received the highest average score (4.6 out of 5), reinforcing the objective performance metrics with practitioner-level consensus. This human-in-the-loop evaluation strengthens the applicability and industrial relevance of the proposed method. In conclusion, the IACO-DWA framework offers superior performance in accuracy, smoothness, path efficiency, and dynamic responsiveness, validating its suitability for current multi-objective path planning scenarios in warehouse robotics and similar domains. Table 3 presents the results.

To ensure the reliability of the experimental results, each simulation configuration was independently repeated 30 times using different random seeds. Key performance metrics presented in Table 1. Table 2 represents the mean values across all trials. Standard deviations (±) for accuracy, RMSE, and success rate were also recorded. For instance, the accuracy of the IACO-DWA model in Table 1 (Experiment A) was 88.4% ± 1.3%, and its RMSE was 0.21 ± 0.02, indicating low variance and stable performance. Furthermore, one-way analysis of variance (ANOVA) tests were conducted across different ablation configurations (Experiments A-E in Table 1), confirming statistically significant differences in accuracy ($p<0.01$) and smoothness score ($p<0.05$). In pairwise comparisons between IACO-DWA and ACO-DWA models, independent t-tests showed that improvements in accuracy, obstacle avoidance success rate, and response time were all significant at the 95% confidence level ($p<0.05$). These results support the conclusion that the proposed model not only provides higher average performance, but also has robust improvements statistically.

The computational complexity of the proposed IACO-DWA algorithm was evaluated in comparison to baseline methods. Standard ACO algorithms typically require repeated global exploration, leading to high computational costs as the number of nodes increases. Although effective in static scenarios, ACO is difficult to achieve real-time response. ACO-DWA has improved this by introducing local path optimization, which accelerates the response in dynamic settings, but introduces additional costs for continuous velocity sampling and path simulation. IACO-DWA further extends this with elite pheromone reinforcement and fuzzy logic evaluation. Although these modules add extra computational layers, their execution is bounded and well-optimized, contributing only minor overhead. As a result, the overall complexity remains manageable and suitable for real-time tasks. In terms of scalability, the experimental results demonstrate that IACO-DWA maintains stable execution efficiency even as the map size and obstacle density increase. On grids up to 200×200, processing time remains within acceptable real-time thresholds. For larger-scale environments, the algorithm design allows for modular upgrades such as resolution adaptation, hierarchical planning, and parallel computation to maintain performance. Therefore, despite the added components, the IACO-DWA algorithm achieves a favorable balance between accuracy, robustness, and computational cost, and can scale to more complex environments without exponential time increase.

5 Discussion

The experimental results reveal that the proposed IACO-DWA model demonstrates significant advantages over existing mainstream methods in warehousing and logistics path planning tasks. Compared with traditional ACO and hybrid ACO-DWA algorithms, IACO-DWA achieves a higher average accuracy (88.4%), shorter path length (15.1m), and lower root mean square error (0.21), while also ensuring a smoother path (smoothness score 0.94) and a higher overall task completion rate (97.3%). Relative to inverse reinforcement learning and deep reinforcement learning methods, which often rely on extensive training data and face latency or generalization challenges in dynamic environments, IACO-DWA avoids these limitations by combining global optimization with real-time adaptability. PRM and NavMesh algorithms perform well in static or structured layouts, but lack responsiveness in high-density, dynamic warehouse spaces, often resulting in long or unstable paths. Optimizers inspired by nature, such as enhanced beetle algorithms, may provide good convergence in complex maps, but often face difficulties in local path smoothing and online adjustment, especially in situations with many obstacles. The improvement of IACO-DWA stems from two key innovations: the elite pheromone reinforcement mechanism accelerates convergence toward high-quality global paths, and the multi-objective fitness function

comprehensively optimizes path length, turning smoothness, and obstacle safety distance. In addition, the dynamic window method integrated at the local level enhances the robot's ability to adjust speed in real-time based on local sensor feedback, ensuring effective obstacle avoidance without losing global directional stability. The ablation results further confirm the contribution of each module, particularly the DWA and elite reinforcement strategies, to system robustness and real-time performance. Overall, the coordinated design of global-local path planning ensures that IACO-DWA can maintain high accuracy and robustness under complex, dynamic warehousing conditions, offering a more adaptive and scalable solution than conventional single-layer or static planning frameworks.

6 Conclusion

Aiming at the insufficient real-time and stability of path planning for warehouse logistics robots in complex environments, a two-level path planning model integrating improved ant colony algorithm and DWA was constructed. In multiple tests with a data volume range of 100 to 1,800, the average accuracy of IACO-DWA reached 88.4%, with an improvement of 14.2% compared to ACO, and the RMSE decreased to 0.21, significantly better than that of ACO (0.48) and ACO-DWA (0.31). In terms of path efficiency, the average path length of IACO-DWA was 15.1m, which was 2.4m shorter than that of ACO. The path smoothness score was 0.94, which was better than that of ACO-DWA (0.85) and ACO (0.63). In terms of dynamic obstacle avoidance capability, IACO-DWA achieved a 96.2% obstacle avoidance success rate, with processing time controlled within 320ms, while ACO processing time was as high as 395ms. In six typical scenario tests, IACO-DWA showed an accuracy close to 0.95 in both Class D and Class F complex environments, with processing time controlled within 250ms, demonstrating good complexity adaptability. Comprehensive analysis shows that the model outperforms existing methods in terms of accuracy, smoothness, robustness, and execution efficiency. However, there is still room for improvement in the collaborative obstacle avoidance ability of the model in high dynamic scenarios. In the future, graph neural networks and multi-objective path prediction models can be combined to further optimize the multi-agent interaction planning ability of paths and expand their application boundaries in large-scale warehousing systems and industrial scenarios.

However, the proposed IACO-DWA algorithm still faces limitations in certain complex navigation environments. In scenarios with dense dynamic obstacles, such as multiple forklifts or moving agents operating simultaneously in confined warehouse zones, the real-time local planning may fail to generate safe and executable trajectories, especially when safe spaces are limited. In narrow corridor-like regions, if the global path generated by IACO fails to fully account for spatial constraints, the robot may experience frequent local oscillations or even be trapped due to insufficient escape width. Furthermore, in environments with severe sensor noise or inaccurate map updates, pheromone information can be misled, causing the system to reinforce sub-optimal or blocked paths. Additionally, as a multi module optimization strategy, the performance of this algorithm is sensitive to the parameter settings of each module. Improper weight values of elite pheromones or fuzzy evaluation rules may lead to unstable paths or overly conservative detours. These failure cases suggest that although IACO-DWA improves performance significantly in structured logistic tasks, further robustness optimization is still needed for highly dynamic, unstructured, or perceptually degraded environments.

References

[1] Priyanka Kumari, and Sudip Kumar Sahana. Heuristic initialization based modified ACO (HIMACO) mimicking ant safety features for multicast routing and its parameter tuning. Microprocessors and Microsystems, 93(9):2-10, 2022. https://doi.org/10.1016/j.micpro.2022.104574

[2] Giacinto Angelo Sgarro, and Luca Grilli. Ant colony optimization for Chinese postman problem. Neural Computing & Applications, 36(6):2901-2920, 2024. https://doi.org/10.1007/s00521-023-09195-4

[3] Zheng Zhang, Juan Chen, and Wenbing Zhao. Multi-AGV route planning in automated warehouse system based on shortest-time Q-learning algorithm. Asian Journal of Control, 5(4):414-419, 2023. https://doi.org/10.1002/asjc.3075

[4] Alireza Shamsoshoara, Fatemeh Lotfi, Sajad Mousavi, Fatemeh Afghah, and İsmail Güvenç. Joint path planning and power allocation of a cellular-connected UAV using apprenticeship learning via deep inverse reinforcement learning. Computer Networks, 254(10):1.1-1.20, 2024. https://doi.org/10.1016/j.comnet.2024.110789

[5] Niloufar Dabestani, Panagiotis Typaldos, Venkata Karteek Yanumula, Ioannis Papamichail, and Markos Papageorgiou. Joint path planning for multiple automated vehicles in lane-free traffic with vehicle nudging. IEEE Transactions on Intelligent Transportation Systems, 25(11):18525-18536, 2024. https://doi.org/10.1109/TITS.2024.3445501

[6] Yushuo Ren, Guoming Zhang, Jianxiang Zheng, and Huifang Miao. An integrated solution for nuclear power plant on-site optimal evacuation path planning based on atmospheric dispersion and dose model. Applied Intelligence, 16(6):1-21, 2024. https://doi.org/10.3390/su16062458

[7] Wanying Zhang, Huajun Zhang, and Xuetao Zhang. An enhanced dung beetle optimizer with adaptive node selection and dynamic step search for mobile robots path planning. Measurement Science and Technology, 36(3):36301.1-36301.15, 2025. https://doi.org/10.1088/1361-6501/adac02

[8] Xianghong Cao, Kunning Wu, Xin Geng, and Yongdong Wang. Indoor fire emergency evacuation path planning based on improved NavMesh algorithm. Journal of Intelligent & Fuzzy Systems,

45(6):10757-10768, 2023. https://doi.org/10.3233/JIFS-232681

[9] Sunil Kumar, and Afzal Sikander. A modified probabilistic roadmap algorithm for efficient mobile robot path planning. Engineering Optimization, 55(9):1616-1634, 2023. https://doi.org/10.1080/0305215X.2022.2104840

[10] Shalini Subramani, and M. Selvi. Intrusion detection system and fuzzy ant colony optimization based secured routing in wireless sensor networks. Soft Computing, 28(18):10345-10367, 2024. https://doi.org/10.1007/s00500-024-09795-9

[11] Khadijeh Nemati, Amir Hosein Refahi Sheikhani, Sohrab Kordrostami, and Kamrad Khoshhal Roudposhti. The embedded feature selection method using ANT colony optimization with structured sparsity norms. Computing, 107(1):1.1-1.22, 2024. https://doi.org/10.1007/s00607-024-01387-7

[12] Bianca Pascariu, Marcella Samà, Paola Pellegrini, Andrea D'Ariano, Joaquin Rodriguez, and Dario Pacciarelli. Effective train routing selection for real-time traffic management: Improved model and ACO parallel computing. Computers & Operations Research, 145(9):2-15, 2022. https://doi.org/10.1016/j.cor.2022.105859

[13] Marco Scianna. The AddACO: A bio-inspired modified version of the ant colony optimization algorithm to solve travel salesman problems. Mathematics and Computers in Simulation, 218(4):357-382. 2024. https://doi.org/10.1016/j.matcom.2023.12.003

[14] Yuelin Gao, Hongguang Wu, and Wanting Wang. A hybrid ant colony optimization with fireworks algorithm to solve capacitated vehicle routing problem. Applied Intelligence: The International Journal of Artificial Intelligence, Neural Networks, and Complex Problem-Solving Technologies, 53(6): 7326-7342, 2023. https://doi.org/10.1007/s10489-022-03912-7

[15] Chetana Hemant Nemade, and Uma Pujeri. Emergency automobile data transmission with ant colony optimization (ACO). Journal of Advances in Information Technology, 15(5):1003-1011, 2023. https://doi.org/10.12720/jait.14.5.1003-1011

[16] Liangang Xie, Xianda Li, and Xiangzhi Wei. A two-layer heterogeneous ant colony system with applications in part-picking planning. Journal of Computing and Information Science in Engineering, 23(2):2-13, 2023. https://doi.org/10.1115/1.4054479